Styrene/2-Ethylhexyl Acrylate/Methacrylic Acid (Sty/EHA/MAA) Coalescence and Response-Driven Mobility of Sodium Dodecyl Sulfate (SDS) in Colloidal Films. 22. A Spectroscopic Study†

W. Reid Dreher, Ping Zhang, and Marek W. Urban*

School of Polymers and High Performance Materials, Shelby F. Thames Polymer Science Research Center, The University of Southern Mississippi, Hattiesburg, Mississippi 39401

R. Shane Porzio and Cheng-Le Zhao

BASF Charlotte Technical Center, BASF Corporation, 11501 Steele Creek Road, Charlotte, North Carolina 28273

Received April 29, 2002

ABSTRACT: The surface morphology of coalesced latex films is a key parameter for understanding coalescence processes and physical and chemical properties of the resulting films. These studies focus on molecular aspects of colloidal film surfaces. Specifically, the distribution and orientation of a commonly used surfactant, sodium dodecyl sulfate (SDS), in films obtained from colloidal dispersions of poly(styrene/ethylhexyl acrylate/methacrylic acid) (Sty/EHA/MAA) and the effect of covalent and ionic entities incorporated into these films are examined. Apparently, the presence of covalently bonded species, such as diacetone acrylamide/adipic dihydrazide (DAAM/ADDH), or ionic species, such as $Ca(OH)_2/NH_4OH$, can effectively immobilize or mobilize SDS molecules during coalescence. Furthermore, molecular orientation of SDS is also influenced causing structural rearrangements near the film−air (F−A) interface. Upon coalescence at 25 °C, the $-SO_3^-Na^+$ moieties take a preferentially parallel orientation, whereas at 60 °C they are randomized. Upon further annealing at 90 °C, $-SO_3^-Na^+$ moieties regain parallel orientation, to become random at 120 °C. This reorganization is affected by the presence of ionic species, H_2O, and cross-linkers to which $SO_3^-Na^+$ groups respond via structural changes from being fully to partially hydrated. Overall, the coalescence of colloidal particles is affected by the presence of minute quantities of active components, which significantly influence surface film morphologies. These studies also show that the response of individual components stimulated by external conditions may lead to specific surface properties and new morphological features.

Introduction

Over the past decade considerable advances in synthesis and analysis allowed us to further understand how colloidal dispersions, particularly after coalescence, may exhibit desirable or undesirable surface and interfacial properties.[1,2] Despite these efforts, there are still a number of issues to be addressed, in particular, understanding of the molecular level conversions of colloidal particles into films. Although several authors have attempted to examine these processes using atomic force microscopy (AFM)[3−5] as well as other techniques,[6,7] these approaches are surface selective methods, thus providing limited information about the bulk and no chemical information. Other attempts to study film formation focused in a polymer component by altering particle morphologies via attaching sizable monomers to a polymer backbone.[8,9] In essence, none of these studies provide chemical information on the film surface during coalescence.

In view of these studies and the fact that only minute chemical changes in particle morphology and/or polymer backbone composition and structure may have extremely significant effects on film formation, the question as to the organization of individual components and the driving forces leading to coalescence is still open. Although one could simplify this scenario and without determining the origin of molecular processes categorize coalescence processes as surface tension or concentration gradient driven entities, this is not the case.[10] For example, recent studies[11,12] clearly indicated that not just commonly accepted polymer attributes, such as the chemical composition of a polymer backbone, molecular weight, or glass transition temperature (T_g), may play a significant role in coalescence. There are a number of often neglected factors which should be considered. Apparently, the presence of other "unimportant", typically low concentration level, components and their usually nonlinear responses to different parameters complicate coalescence. While these complexities raise a number of scientific challenges and questions, they also open up a number of opportunities and ultimately exhibit very important practical implications. For example, there are significant differences in surface properties between colloidal dispersions prepared from copolymers and blends of the same monomers, or the presence of different stabilizing agents may alter coalescence, or the pH of an aqueous phase for the same particle morphologies may alter surface characteristics of coalesced films.[11,12] These issues become even more complicated when one considers differences in particle surface morphologies such as carboxylic acid or other reactive groups that may result in cross-linked networks interpenetrating high molecular weight thermoplastic macromolecules.[13] Previous studies[13] on EA/MAA and Sty/nBA[11,13] dispersions showed that probably the most efficient way to tackle these complex processes is to

* To whom all correspondence should be addressed.

† Parts 1−21 were published in *Macromolecules* and *J. Appl. Polym. Sci.*

10.1021/ma020663w CCC: $25.00
Published on Web 01/30/2003

either sanitize colloidal dispersions from low molecular weight components and focus strictly on particle deformation during coalescence or utilize experimental approaches that allow nondestructive analysis in the presence of all components. While the latter is our preference, studies by Scriven et al.[14] illustrated an elegant way of utilizing freeze−fracture methods for the analysis of coalescence. Using cryogenic methods combined with scanning electron microscopy (SEM) along with the precise control of particle size and its chemical makeup, theses studies revealed that the capillary forces and pressure from the surface tension in curved menisci as well as contact lines dominate stresses, deformation, and flattening of surface particles, ultimately leading to coalescence. If this is the case, surface-active components such as surfactants and other non-chemically-bonded species will play a significant role in the development of surface morphologies during coalescence.

With this in mind and considering recent[15,16] developments, let us consider a multi − component system, such as 2-ethylhexyl acrylate (EHA) copolymerized with styrene (Sty) and methacrylic acid (MAA) to form Sty/EHA/MAA copolymer particles and attempt to understand their behavior under different stimuli conditions. Specifically, the effect of additives on molecular level processes of Sty/EHA/MAA colloidal dispersions which contain nonionic and ionic species purposely introduced in order to alter colloidal particle environments and influence ionic/nonionic interactions with the Sty/EHA/MAA dispersion will be examined. This is particularly important because the previous studies,[17] which focused on the behavior of surfactants and the effect of colloidal particle morphologies on film formation, recognized that often low concentration levels of "insignificant" components may play an important role in the film formation.

Experimental Section

Styrene (Sty), 2-ethylhexyl acrylate (EHA), methacrylic acid (MAA), diacetoneacrylamide (DAAM), adipic hydrazide (ADDH), sodium dodecyl sulfate (SDS), calcium hydroxide ($Ca(OH)_2$), calcium chloride ($CaCl_2$), and ammonium hydroxide (NH_4OH) were purchased from Aldrich Chemical Co. For model studies, the designated molar ratios of each compound were dissolved in double deionize (DDI) water, and such prepared solutions were analyzed spectroscopically. Sty/EHA/MAA colloidal dispersions were synthesized by a semicontinuous polymerization process reported elsewhere.[18] Sty/EHA/MAA dispersions were cast on a poly(vinyl chloride) (PVC) substrate and allowed to coalesce at 50% relative humidity (RH) for 3 days at 24 °C to form approximately 50 μm thick films. Such prepared films were annealed at 60, 90, and 120 °C for 2 h.

Polarized attenuated total reflectance Fourier transform infrared (ATR FT-IR) spectra were collected using a Bio-Rad FTS-6000 FT-IR single-beam spectrometer set at a 4 cm^{-1} resolution equipped with a ZnSe polarizer. A 45° face angle Ge crystal with 50 × 20 × 3 mm dimensions was used. This configuration allows the analysis of the film−air (F−A) interface at approximately 0.2 μm from the surfaces. The use of a ZnSe polarizer facilitates orientation studies by utilizing TE (transverse electric) and TM (transverse magnetic) modes of polarized IR light. Each spectrum represents 100 co-added scans ratioed against the same number of reference scans collected using an empty ATR cell. All spectra were corrected for spectral distortions and optical effects using Q-ATR software.[19]

Vibrational energies of $SO_4^-Na^+$ ends of SDS exposed to different ionic environments were theoretically predicted using the HyperChem software package (Hypercube, Inc.), which utilized ab initio quantum mechanical calculations by incorporating the 6-31G* basis set. These atomic force microscopy images were collected using a Nanoscope IIIa Dimension 3000 scanning probe microscope (Digital Instruments) set at the resonance frequency of 310 kHz equipped with a Si cantilever.

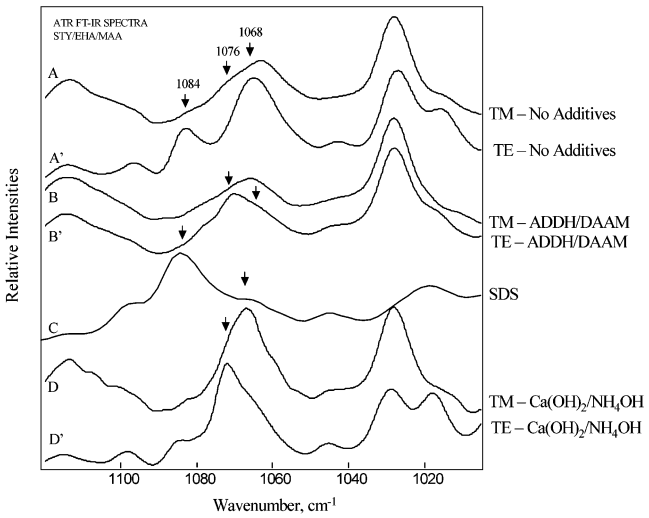

Figure 1. Polarized ATR FT-IR spectra of Sty/EHA/MAA recorded from the F−A interface: A and A′, TM and TE polarizations of pure Sty/EHA/MAA; B and B′, TM and TE polarization of Sty/EHA/MAA containing DAAM and ADDH; C, SDS; D and D′, TM and TE polarization of Sty/EHA/MAA containing the ionic species $Ca(OH)_2$ and NH_4OH.

Results and Discussion

The presence of various components in polymeric dispersions plays an important role in the stabilization of colloidal particles. For example, it is well-known that introducing cross-linkable moieties may reinforce colloidal polymer networks and likely alter mobility of species that are not chemically affixed to a polymer matrix. Furthermore, as a result of surface morphological changes, orientation of surface species may be altered. As a matter of fact, previous studies[16] concerning SDOSS and SDS behavior in Sty/nBA/MAA revealed that while hydrophobic chains are preferentially perpendicular to the surface, their hydrophilic ends ($-SO_3^-Na^+$) associated with H_2O and −COOH entities tend to align parallel to the film surface,[16] and the S−O bond of the $-SO_3^-Na^+$ group of SDOSS or SDS can take either out-of-plane or in-plane conformations, depending on their environments. Thus, there is a significant effect of how given molecular moieties are going to respond to chemical environments during or after coalescence.

With this in mind let us consider Sty/EHA/MAA films coalesced at 25 °C/50% RH, and utilize ATR FT-IR measurements as a proven method for molecular level information at about 0.18 μm from the surface. Traces A and A′ of Figure 1 illustrate polarized ATR FT-IR spectra recorded from the F−A interface. While trace A was recorded using TM polarization, trace A′ represents the TE mode. As seen, there are significant differences between these spectra which are demonstrated by the intensity changes of the bands at 1084 and 1068 cm^{-1}. Although these changes reflect preferential orientation of molecular entities responsible for these bands, before we establish the origin of these changes, let us consider traces B and B′ of Figure 1 which also illustrates TM and TE ATR FT-IR spectra of the same film. In this case DAAM and ADDH were used to cross-link films of Sty/EHA/MAA copolymer dispersion via the ketohydrazide cross-linking mecha-

nism.[18] It is quite apparent that there are significant differences between spectral pairs A/A′ and B/B′ that are reflected not only in the intensity changes but also in the appearance of a new band at 1076 cm^{-1} when TE polarization is employed. In contrast, when TM polarization is used, the 1068 cm^{-1} is detected (trace B). Comparison of the above data with the SDS transmission spectrum shown in trace C, Figure 1, indicates that only one band at 1084 cm^{-1} due to the S−O stretching vibrations of the $-SO_3^-Na^+$ hydrophilic end is detected for pure SDS. However, when SDS is placed into the Sty/EHA/MAA polymer matrix environment containing ionic and nonionic species, there are significant changes in the S−O energies, thus confirming its responsiveness to chemical environments. It should be noted that the amount of DAAM and ADDH represent only 1.5 w/w % with respect to the total amount of all the monomers.

At this point three questions need to be addressed: (1) why SDS diffuses to the F−A interface, as evidenced by the presence of the 1084 cm^{-1} band; 2) why the $-SO_3^-Na^+$ entities exhibit preferential orientation, as demonstrated in Figure 1, traces A and A′; (3) what chemical/physical changes are responsible for the 1068 and 1076 cm^{-1} bands, as evidenced by traces A and A′. To address these issues let us first consider how the $-SO_3^-Na^+$ environment may be disturbed by the presence of electron donors or acceptors. For that reason 0.25 w/w % of $Ca(OH)_2$ and 0.25 w/w % of NH_4OH were added to Sty/EHA/MAA aqueous colloidal dispersions and following their coalescence, such films were analyzed spectroscopically. Traces D and D′ of Figure 1 illustrate TM and TE polarized ATR FT-IR spectra recorded from the F−A interface. It is apparent that the 1068 cm^{-1} band dominates the spectrum when TM polarization is used, whereas for TE polarization, the 1076 cm^{-1} band is present. It should be also noted that trace D also features the bands at 1084 and 1076 cm^{-1} and a shoulder at 1068 cm^{-1}. Thus, these data indicate that, by the addition of ionic species, the $-SO_3^-Na^+$ environment is altered, and the S−O stretching vibrational energy changes from 1084 to 1068 and 1076 cm^{-1}.

Postponing temporarily the discussion concerning the origin of these apparent changes induced by ionic environments and the mobility of SDS to the F−A interface, let us attempt to address the origin of preferential surface orientation. As shown in trace D of Figure 1, the 1068 cm^{-1} band dominates this spectral region, but when TE polarization is employed (Figure 1, trace D′), the band at 1076 cm^{-1} is detected, thus indicating substantial orientation changes. To address the origin of these changes we conducted a series of model studies, in which we altered the SDS environment near the F−A interface. The results are shown in Figure 2. While trace A is the IR spectrum of $Ca(OH)_2$, traces B−H represent different concentration levels and conditions to which SDS was subjected. First, SDS was heated to 50 °C for 3 days and the resulting spectrum is shown in Figure 2C. For reference, trace B is the SDS spectrum recorded at room temperature. In both spectra the 1084 cm^{-1} band is detected indicating that the temperature changes has a minimal effect on the $-SO_3^-Na^+$ environment, although an already weak 1068 cm^{-1} band intensity diminishes to a minimum after heating at 50 °C. This behavior is most likely attributed to the $-SO_3^-Na^+\cdots H_2O$ interactions, as similar situations were observed for SDOSS,[15] where

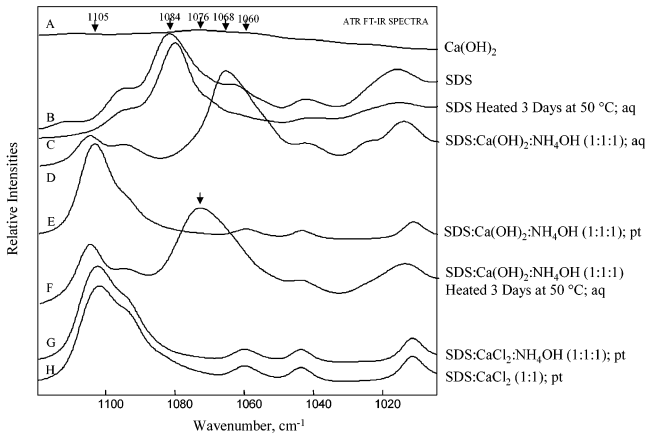

Figure 2. ATR FT-IR spectra: A, $Ca(OH)_2$; B, SDS; C, SDS heated 3 days at 50 °C; D, SDS:$Ca(OH)_2$:NH_4OH (1:1:1) mixture from an aqueous phase; E, SDS:$Ca(OH)_2$:NH_4OH (1:1:1) precipitate from an aqueous phase; F, SDS:$Ca(OH)_2$:NH_4OH (1:1:1) mixture from an aqueous phase heated 3 days at 50 °C; G, SDS:$CaCl_2$:NH_4OH (1:1:1) precipitate from an aqueous phase; H, SDS:$CaCl_2$(1:1) precipitate from an aqueous phase.

the band at 1050 cm^{-1} due to S−O stretching vibrations resulted in the appearance of two bands at 1056 and 1046 cm^{-1} due to COOH and H_2O interactions, respectively.

As shown in Figure 1, as a result of addition of $Ca(OH)_2$ and NH_4OH, bands at 1068 and 1076 cm^{-1} were detected. In an effort to determine the origin of these bands and ultimately the molecular entities responsible for these bands, we prepared a series of solution/solid mixtures containing SDS/$Ca(OH)_2$/NH_4OH species. Traces D and E of Figure 2 illustrate FT-IR spectra of SDS/$Ca(OH)_2$/NH_4OH in 1:1:1 molar ratios which was used in preparing Sty/EHA/MAA emulsions (Figure 1, parts D and D′). In this case, an aqueous solution as well as the precipitate of the three components was analyzed, as $Ca(OH)_2$ has limited water solubility. The results are shown in Figure 2, traces D and E, respectively, which illustrate that the bands at 1068 and 1076 cm^{-1} increase. At the same time the band at 1084 cm^{-1} is not detected, but a new band at 1105 cm^{-1} is present, thus indicating that there is a substantial difference between chemical compositions of an aqueous aliquot and the precipitate. The presence of the 1068 cm^{-1} band clearly indicates that, in the presence of water and $Ca(OH)_2$, the S−O stretching band shifts to 1068 cm^{-1}. Going one step further, when SDS/$Ca(OH)_2$/NH_4OH mixture (trace D) was heated for 3 days at 50 °C and analyzed, trace F resulted. As seen, the band at 1068 cm^{-1} diminishes to minimum at the expense of the 1076 cm^{-1} that dominates the spectrum. On the basis of this analysis it is quite clear that this process essentially removes NH_3 and H_2O from the mixture and the new band at 1076 cm^{-1}, resulting from $-SO_3^-Na^+$ and $Ca(OH)_2$ interactions, is detected. As Ca^{2+} and OH^- moieties in the presence of NH_4OH and H_2O approach hydrophilic $-SO_3^-Na^+$ groups of SDS, the $-SO_3^-Na^+$ environment is disturbed and orientation changes occur. As we recall, the 1068 cm^{-1} band was detected using TM polarization (trace D, Figure 2) and the 1076 cm^{-1} band along with the shoulders at 1068 and 1084 cm^{-1} is detected for TE polarization (trace D′, Figure 2).

In an effort to further understand conformational changes of $-SO_3^-Na^+$ groups, we utilized ab initio quantum mechanical calculations which employed the 6-31G* basis set to predict vibrational energies associ-

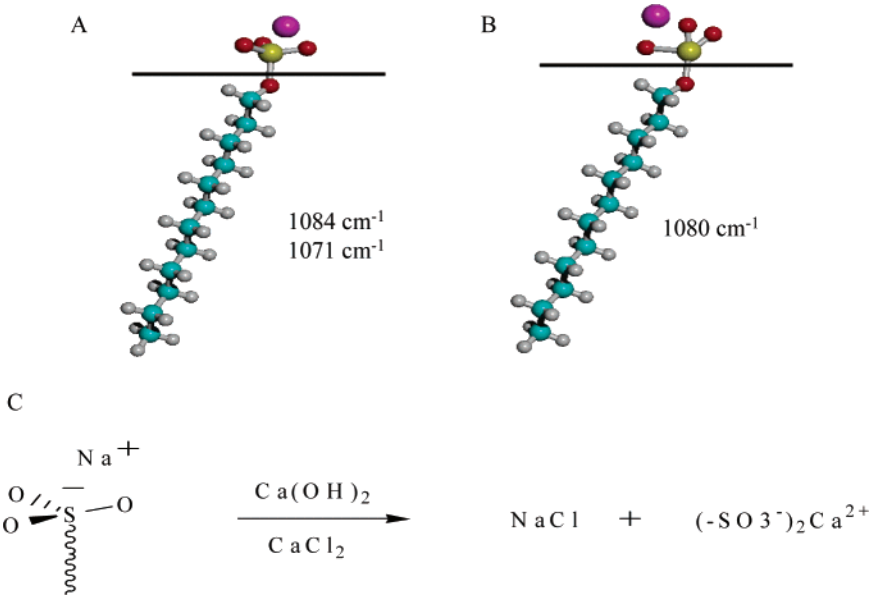

Figure 3. Preferential orientation of $-SO_3^-Na^+$ groups on the surface of the latex films: A, $-SO_3^-Na^+$ preferentially parallel; B, $-SO_3^-Na^+$ preferentially perpendicular; C, $-SO_3^-Na^+$ disrupted by the presence of $Ca(OH)_2/CaCl_2$.

ated with the S−O stretching vibrations of SDS and its response to different environments. This was accomplished by altering the geometry of the $-SO_3^-Na^+$ entity (bond length and bond angles) to match experimentally determined S−O stretching vibrations in the 1060−1090 cm^{-1} range. Using this approach, the $-SO_3^-Na^+$ structures depicted in Figure 3, parts A and B, were obtained. While structure A generates the 1084 and 1071 cm^{-1} bands, structure B is responsible for a single band at 1080 cm^{-1}. For structure A, when the three exterior oxygens are arranged in the same plane as the sulfur atom, or S−O bonds are parallel to the surface, two IR active bands due to asymmetric vibrations are present. However, as shown in Figure 3B, as one of the oxygens is removed from the plane and takes preferentially perpendicular orientation to the surface, only one band is IR active. These results closely match the experimental data, and indicate that the position of the Na^+ cation with respect to the $-SO_3^-$ geometry is altered by the presence of Ca^{2+} ions.

As previous experiments indicated, the presence of H_2O may significantly alter the SDS interfacial behavior. Specifically, the degree of hydration of SDS can be highly influenced not only by the H_2O content, but the presence of other hydroscopic ionic species which, due to their different hydroscopic nature, may carry different water contents. Since the SDS crystalline size is significantly affected by the amount of water, its crystalline structure changes. For example, depending on the degree of hydration, the average area per polar headgroup steadily changes from 19.3 to 29.5 $Å^2$ when going from SDS to SDS·H_2O.[20] At the same time, the lamellar thickness diminishes from 19.43 to 14.41 Å. In contrast, the angle between long axis of the SDS anion and unit cell can fluctuate from 15° for SDS to 40 and 45° for SDS·$^1/_2H_2O$ and SDS·H_2O, respectively.[20] Partial hydration of SDS to form SDS·$^1/_8H_2O$ leads to a 5° angle, thus resulting in preferential parallel orientation with respect to the F−A interface. To even further alter ionic environments between $-SO_3^-Na^+$ and $Ca(OH)_2$, $CaCl_2$ was introduced, and as illustrated by traces G and H of Figure 2, the detected spectral features are almost identical to trace E of Figure 2, indicating that the

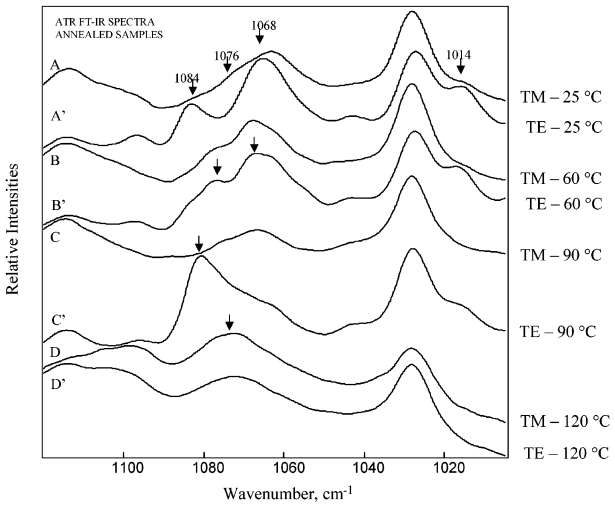

Figure 4. Annealing experiments of thin films from p-Sty/EHA/MAA dispersions on PVC substrate at different temperatures: A, 25 °C, TM; A′, 25 °C, TE; B, 60 °C, TM; B′, 60 °C, TE; C, 90 °C, TM, C′, 90 °C, TE; D, 120 °C, TM; D′, 120 °C, TE.

$-SO_3^-Na^+$ groups react with $CaCl_2$ to form NaCl and $Ca^{2+}(-SO_3^-)_2$ precipitate, with the solution containing nonprecipitated $Ca(OH)_2$. The presence of the Ca^{2+}-$(-OSO3^-)_2$ precipitate is represented by the presence of the 1105 cm^{-1} band, as shown in trace F of Figure 2.

Using the model experiments depicted above, the origin of the orientation and the chemical processes responsible for specific bands allowed us to understand the origin of ionic interactions. However, the origin of the SDS diffusion is not apparent. One could speculate that the water flux combined with the SDS compatibility with the polymer matrix may play a significant role, but as previously indicated, annealing at elevated temperatures does not alter mobility to the FA interface. Nevertheless, morphological surface features change.[13] For that reason we conducted a series of temperature experiments that are described below. As shown in Figure 4, traces A and A′ indicate that two bands at 1084 and 1068 cm^{-1} dominate the spectral region when the spectra are collected using TE polarizations at 25

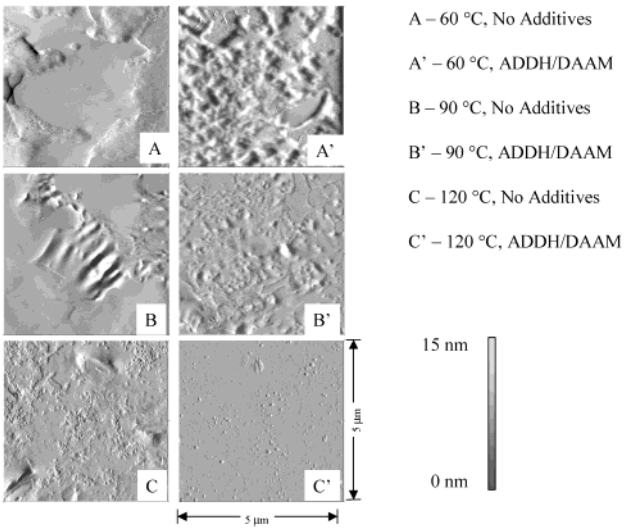

Figure 5. AFM amplitude images of thin films from p-Sty/EHA/MAA dispersions annealed at elevated temperatures: A, no additives, 60 °C; A′, ADDH/DAAM, 60 °C; B, no additives, 90 °C; B′, ADDH/DAAM, 90 °C; C, no additives, 120 °C; C′, ADDH/DAAM, 120 °C, respectively. The scan box size was 5 μm and the contrast for the amplitude images covers 15 (A), 10 (A′), 20 (B), 10 (B′), 5 (C), and 10 nm (C′).

°C. When the same specimen is annealed at 60 °C, it is quite apparent that the band at 1084 cm^{-1} diminishes at the expense of the 1076 and 1068 cm^{-1} bands. This is illustrated in Figure 4, traces B and B′, and further annealing at 90 °C results in substantial differences of the TE and TM spectra, as shown by traces C and C′ in Figure 4. When the spectra are collected using TE polarization, the band at 1084 cm^{-1} becomes very intense, and at the same time, this band is not present for TM polarization. Annealing at 120 °C results in TE and TM polarizations with no intensity differences, thus indicating random orientation of the surface species.

Specimens annealed at 25 °C produced the same spectral features as described in Figure 1, traces A and A′, indicating that there is preferential orientation of the $-SO_3^-Na^+$ moieties near the F−A interface. As we recall, when the ADDH/DAAM cross-linking system was incorporated as part of the aqueous colloidal dispersion, there was limited diffusion to the F−A interface (Figure 1, traces B and B′), thus indicating that the presence of the cross-linkers not only reinforces the matrix, but also physically inhibits the mobility of low molecular weight species to the F−A interface. However, the mobility of SDS to the F−A interface is mostly affected by altering SDS environments due to its response to chemically or thermally induced processes.

In view of the above discussion and the results presented in Figure 4, let us consider surface morphological changes resulting from temperature responses. While Figure 5A is an AFM image of the surface of Sty/EHA/MAA annealed at 60 °C, image A′ illustrates its counterpart containing ADDH/DAAM cross-linkers. As seen, it is quite apparent that the surface of the film without cross-linkers (A) is significantly smoother, indicating that, under these experimental conditions, interdiffusion of particles occurs. In contrast, when the ADDH/DAAM was employed, its presence slows down the coalescence process, which is manifested by the AFM image with significantly irregular surface features. Combining the above data with the spectral information (Figure 4, parts B and B′) obtained for the same specimens indicate that, at 60 °C, the $-SO_3^-Na^+$ groups become random, as illustrated by unchanging intensities of the normal vibrations due to S−O recorded using TE and TM polarizations.

To examine if the particle flow occurs in the presence of cross-linkers, elevated temperatures were employed, and Figure 5, parts B/B′ and C/C′, illustrates the resulting AFM images. As shown, when Sty/EHA/MAA films containing cross-linkers were annealed at 90 °C, coalescence occurred to greater extent, which is evidenced by a smoother surface. However, at the same time, the presence of SDS at the F−A interface exhibits interesting features. As illustrated in Figure 4, parts C and C′, there are drastic intensity changes between TM (C) and TE (C′) polarizations, thus indicating that at this temperature the $-SO_3^-Na^+$ groups are preferentially parallel to the surface. This observation fits the model predicted in Figure 3, A, with two asymmetric vibrations at 1074 and 1081 cm^{-1}, but the 1081 cm^{-1} band is significantly stronger. When the same specimens were annealed at 120 °C, a smooth surface was obtained, as manifested by the AFM images illustrated in Figure 5, parts C and C′, indicating that at that temperature particle flow has occurred. At the same time, $-SO_3^-Na^+$ moieties were randomized, as detected spectroscopically in Figure 4, traces D and D′, with no intensity differences between TE and TM polarizations.

Ionic environments generated by the presence of surfactant and other ionic species impose another question: what is the role of MAA monomer, if any, in these interactions. Previous studies indicated that for sodium dioctylsulfosuccinate (SDOSS) surfactant, $SO_3^-Na^+$ groups are sensitive to acid and water environments. Apparently, this is not the case for this system, and analysis of the F−A interfaces showed no indication of S−O···COOH interactions. These observations indicate that MAA monomer is incorporated inside the particles and does not migrate to the F−A interface during coalescence.

In view of the above considerations, the following scenario shown in Figure 6 can be depicted for the film formation of Sty/EHA/MAA model dispersions in the presence of covalently and ionically bonded cross-linkers. As shown in Figure 6A, for the virgin Sty/EHA/MAA dispersions, SDS forms oriented surface domains with $-SO_3^-Na^+$ moieties preferentially parallel to the surface. However, when ADDH/DAAM cross-linkers are incorporated into Sty/EHA/MAA dispersions, limited diffusion of SDS to the surface occurs and the particle flow occurs at elevated temperatures. This is illustrated in Figure 6B. Apparently, balance between surfactant mobility, cross-linking, particle interdiffusion, and environmental response of individual components leads to specific surface morphologies. The entire process becomes even more complex when ionic species are incorporated resulting in SDS structural changes depicted in Figure 6C. Upon coalescence at 25 °C, the $-SO_3^-Na^+$ moieties take preferentially parallel orientation, and at 60 °C, they are randomized. Upon further annealing at 90 °C, $-SO_3^-Na^+$ moieties regain preferential parallel orientation, followed by their randomization at 120 °C. Reorganization of SDS is clearly affected by the presence of ionic species, H_2O, and cross-linkers to which $SO_3^-Na^+$ groups respond via structural changes fully to partially hydrated SDS·H_2O. As a result, the position of the Na^+ ions with respect to the SO_3^- groups

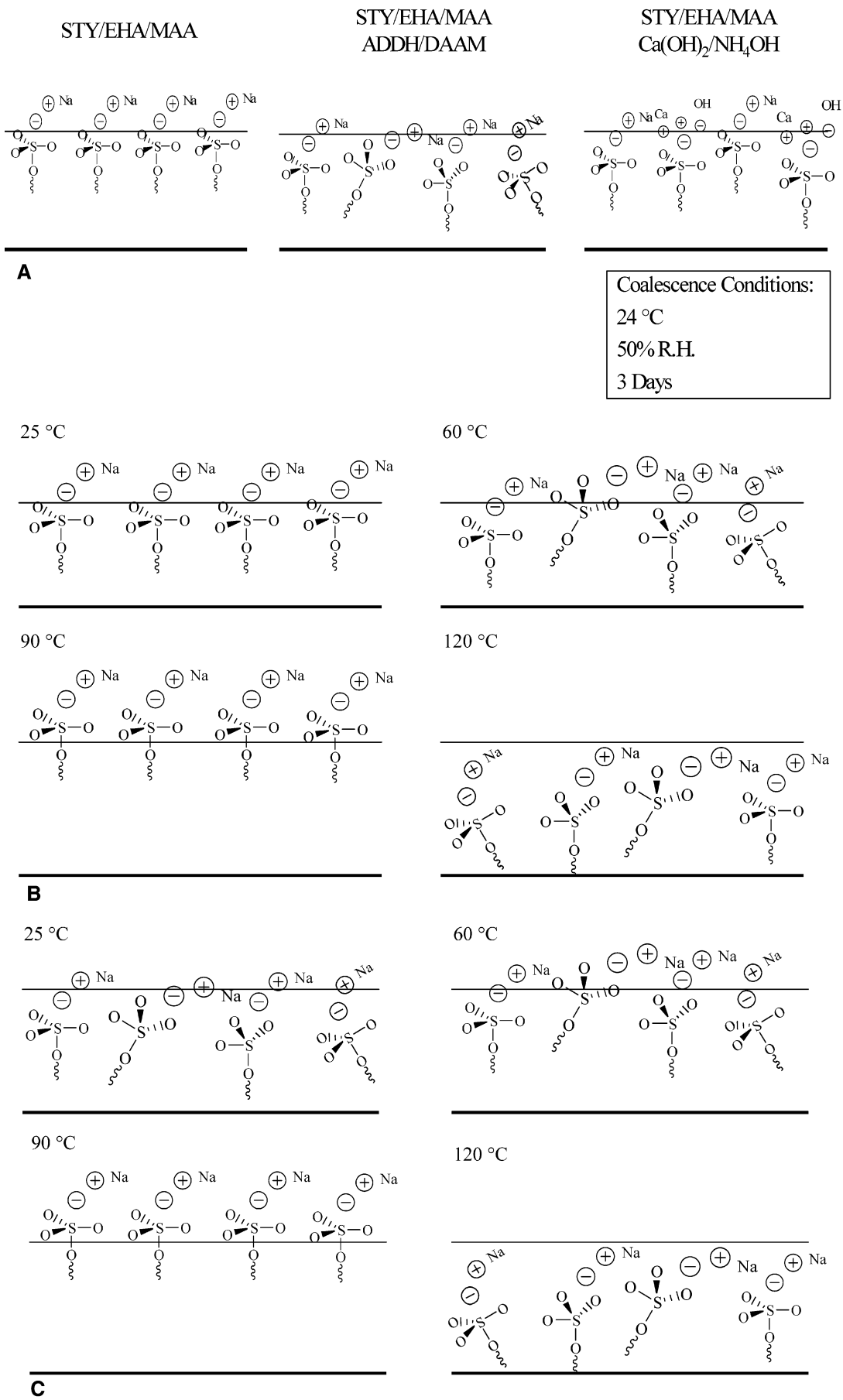

Figure 6. Pictorial representation of orientation and distribution of SDS molecules near the F−A interface (see text for description).

changes, ultimately leading to the intensity and vibrational energy changes depicted in Figure 4.

Conclusions

Film formation processes resulting from coalescence of Sty/EHA/MAA colloidal dispersions are affected by the presence of low level covalently and ionically cross-linking species. Neat Sty/EHA/MAA dispersions are able to coalesce at room-temperature conditions, as illustrated by the smoothness surface as an indicator and the presence of SDS at the F−A interface. However, dispersions containing ADDH/DAAM cross-linking agents coalesce slower, and elevated temperatures are required for complete particle coalescence. The presence of ionic species such as $Ca(OH)_2$ and NH_4OH does not effect the coalesce of particles, but orientation and/or migration of surfactant molecules are altered. ATR FT-IR polarization experiments along with ab initio quantum mechanical calculations show that the hydrophilic $-SO_3^-Na^+$ groups of SDS are preferentially parallel near the F − A interface. These studies also show that it is possible to control responses of SDS using minute quantities of ionic species that alter $-SO_3^-Na^+$ conformational features near the F−A interface. Finally, competing processes between mobility of individual components, particle coalescence, cross-linking, and physicochemical environments affect film formation processes.

Acknowledgment. The authors are thankful to BASF Corp. for financial support of these studies. Partial support for these studies (W.R.D. and M.W.U.) from the National Science Foundation Materials Research Science and Engineering Center (DMR 0213883) at the University of Southern Mississippi is also acknowledged.

References and Notes

(1) Lovell, P. A.; El-Aasser, M. S. *Emulsion Polymerization and Emulsion Polymers*; John Wiley & Sons: New York, 1997.
(2) Urban, M. W.; Provder, T. *Film Formation*; ACS Symposium Series 790; American Chemical Society: Washington, DC, 2002.
(3) Linemann, R.; Malner, T.; Brandsch, R.; Bar, G.; Ritter, W.; Mulhaupt, R. *Macromolecules* **1999**, *32*, 1715.
(4) Thomas, R.; Lloyd, K.; Stika, K.; Stephans, L.; Magallanes, V.; Sudol, E.; El-Aasser, M. *Macromolecules* **2000**, *33*, 8828.
(5) Cannon, L.; Pethrick, R. *Polymer* **2001**, *43*, 1223.
(6) Marion, P.; Beinert, G.; Juhue, D.; Lang, J. *J. Appl. Polym. Sci.* **1997**, *64*, 2409.
(7) Marion, P.; Beinert, G.; Juhue, D.; Lang, J. *Macromolecules* **1997**, *30*, 123.
(8) Zhao, C.; Wang, Y.; Hruska, Z.; Winnik, M. *Macromolecules* **1990**, *23*, 4082.
(9) Liu, Y.; Feng, J.; Winnik, M. *J. Chem. Phys.* **1994**, *101*, 9096.
(10) Holl, Y.; Veddie, J. L.; McDonald, P. J.; Winnik, M. A. In *Film Formation in Coatings*; ACS Symposium Series 790; American Chemical Society: Washington, DC, 2001.
(11) Zhao, Y.; Urban, M. W. *Macromolecules* **2000**, *33*, 2184.
(12) Zhao, Y.; Urban, M. W. *Macromolecules* **2000**, *33*, 8426.
(13) Zhao, Y.; Urban, M. W. *Macromolecules* **2000**, *33*, 7573.
(14) Pekurovsky, L.; Scriven, L. *On Capillary Forces and Stress in Drying Latex Coating*; Urban, M. W., Provder, T., Eds.; ACS Symposium Series 790; American Chemical Society: Washington DC, 2001.
(15) Zhao, Y.; Urban, M. W. *Langmuir* **2000**, *16*, 9439.
(16) Zhao, Y.; Urban, M. W. *Langmuir* **2001**, *17*, 6961.
(17) Zhang, P.; Smith, O.; Thames, S. F.; Urban, M. W. Manuscript in preparation.
(18) Zhao, C.; Wistuba, E.; Roser, J.; Fitzgerald, P.; Spitzer, J. In US Patent 6,242,515, 2001.
(19) Urban, M. W. *Attenuated Total Reflectance Spectroscopy of Polymers Theory and Practice*; American Chemical Society: Washington, DC, 1996.
(20) Smith, L. A.; Hammond, R. B.; Roberts, K. J.; Machin, D.; McLeod, G. *J. Mol. Struct.* **2000**, *554*, 173.

MA020663W